

Ultra - High Energy Cosmic Rays from decay of the Super Heavy Dark Matter Relics.

A.G. Doroshkevich

Theoretical Astrophysics Center, Juliane Maries Vej 30, 2100 Copenhagen, Ø Denmark;

P.D. Naselsky

Theoretical Astrophysics Center, Juliane Maries Vej 30, 2100 Copenhagen, Ø Denmark;

Rostov State University, Zorge 5, 344090, Rostov-Don, Russia

In this paper we briefly discuss the problem of the origin of Ultra High Energy Cosmic Rays in the framework of Top-Down models. We show that, for high energy of decays and in a wide range of spectra of injected protons, their extragalactic flux is consistent with the observed fluxes of cosmic rays in the energy range $0.1E_{GZK} \leq E \leq 10E_{GZK}$. For suitable energy and spectra of injected protons, the contribution of galactic sources is moderate, in this energy range, but it dominates at smaller and larger energies. In such models we can expect that at these energies the anisotropy of cosmic rays distribution over sky will be especially small.

Some possible manifestations of decays of super massive particles such as, for example, primordial black holes with masses $M_{pbh} \sim 10^{-5}g$, are considered. In particular, we show that partial conversion of energy released during these decays at redshifts $z \sim 1000$ to Ly- α photons can delay the hydrogen recombination and distort the spectrum of fluctuations of the cosmic microwave background radiation.

PACS number(s): 98.80.Cq, 95.35.+d, 97.60.Lf, 98.70.Vc.

I. INTRODUCTION

The origin of Ultra - High Energy Cosmic Rays (UHECR) with energy above the Greisen-Zatsepin-Kuzmin (GZK) [1,2] cutoff, $E_{GZK} \sim 10^{20}$ eV, is one of the most intriguing mysteries of the modern physics and astrophysics. After the pioneering papers [1,2] and recent observations of the UHECR energy power spectra by AGASA [3], Fly's Eye [4] and Haverah Park [5], several possible mechanisms of the UHECR production were discussed (see reviews [6,7]).

In this paper we consider the so-called Top-Down scenario of the UHECR creation which is associated with decays of Super Heavy Dark Matter (SHDM) particles with masses $m_{SHDM} > 10^{12}$ GeV. This mechanism was for the first time suggested by Berezhinsky, Kachelrieß and Vilenkin [8] (see also [9]) and now it seems to be a natural way of explaining the origin of UHECR with energies above the GZK cutoff.

Several kinds of SHDM particles which could be created in the early Universe are discussed in literature. Particles with masses of about one to two orders of magnitude larger than the typical mass of inflaton, $m_\phi \sim 10^{13}$

GeV, could be very efficiently created at the preheating phase of inflation [11]. SHDM particles can also be related to topological defects, such as strings [12,13], magnetic monopoles [14,15], necklaces [16] and vortons [17].

The possible contribution of primordial black hole relics (PBHs) to the dark matter (DM) were discussed already in [18] and [19]. Recently Dolgov, Naselsky and Novikov [20] considered PBHs with masses $M_{PBH} \sim 10^6$ g as possible sources of the baryonic asymmetry and the high entropy of the Universe. They assume that remnants of such black holes with masses of about Planck mass survive up to now and form the SHDM relics. Mergers of these remnants within high density clumps creates more massive black holes, stimulates their explosive evaporation and could produce ultra-high energy particles observed as rare UHECRs.

This discussion shows that, in the framework of the Top-Down scenario, the UHECR can be related to various kinds of SHDM particles with masses $10^{12} \leq m_X \leq 10^{19}$ GeV. (Below by X we denote all possible types of SHDM).

Now the possible energy losses of the UHECR are well established [21] and observational predictions of the Top-Down scenario of the UHECR creation crucially depend upon unknown factors such as the mass of the SHDM particles, energy spectrum and composition of decay products. It is commonly believed, that the observed UHECR spectrum at both $E \leq E_{GZK}$ and $E \geq E_{GZK}$ is dominated mainly by local sources and it simply reproduces the spectra of injected protons. However, at energies $E \sim E_{GZK}$, the complex shape of observed UHECR fluxes shows that it can be more sensitive to extragalactic component of high energy protons and, so, can depend upon the unknown factors mentioned above. Detailed investigation of the spectrum and anisotropy of UHECR in the range $E/E_{GZK} \geq 0.1$ can discriminate between discussed versions of the Top-Down models and restrict some parameters of the SHDM particles and the process of proton creation.

As is commonly believed, decays of SHDM particles into the high energy protons, photons, electron-positron pairs and neutrinos occurs through the production of quark-antiquark pairs ($X \rightarrow q, \bar{q}$), which rapidly hadronize and generate two jets and transform the en-

ergy into pions ($\sim 95\%$) and hadrons ($\sim 5\%$) [21]. It can be expected that later most of that energy is transformed into high energy photons and neutrinos with the energy spectrum $S(E) \propto E^{-1.5}$, at $E \ll M_X$ [21]. Similar spectrum for the hadronic component is also expected. This means that, for such decays of SHDM particles with $10^{12} < m_X < 10^{19}$ GeV, the UHECR with energies $E > 10^{20}$ eV are dominated by photons and neutrinos [21]. This conclusion can be tested with further observations of the UHECR fluxes at $E > 10^{20}$ eV.

Other spectra of protons generated by decays of SHDM particles are also discussed. In particular, such spectrum can be similar to Gaussian or δ -function centered at $E_X \sim m_X \gg 10^{20}$ eV. In this case the spectrum of protons created by nearby sources will be also similar to the same δ -function while the spectrum of the extragalactic component is $\propto E^{-1}$ at both $E < E_{GZK}$ and $E > E_{GZK}$ and is consistent with the observed one at $E \sim E_{GZK}$.

Recently Berezhinsky and Kachelrieß [13] discussed Monte Carlo simulations of the jet fragmentation in SUSY-QCD. They found that the spectrum of injected protons can be well fitted to log-normal distribution. Farrar and Piran [23] discussed the spectrum of injected protons $S(E) \propto E^{-\alpha}$, with $0 < \alpha \leq 1$ in the Top-Down model of the UHECR origin. We show that, for such spectra, the flux of extragalactic protons at $E \sim E_{GZK}$ is also consistent with the observed one.

Another important factor is the observed anisotropy of the UHECR distribution over the sky. As was discussed by Berezhinsky et al. [8], both CDM and SHDM particles are clustered within galactic halos and their decays inevitably generate some anisotropy. In particular, if the contribution of Galactic sources dominates we will see an anisotropy of the UHECR due to our asymmetric position in the Galaxy. In contrast, the extragalactic component of UHECRs is averaged over the volume with a size ≥ 50 Mpc and its angular distribution is almost isotropic. The contributions of closest galaxies and the Local Supercluster of galaxies could also be observed.

The relative contributions of Galactic and extragalactic UHECRs sources depend upon many unknown factors such as the size of galactic halo, overdensity and spatial distribution of SHDM particles within the halo [6]. However, for larger energy of injection, $E_{inj} \geq 10^4 - 10^5 E_{GZK}$, and for Gaussian, log-normal and power spectra of injected protons with $\alpha \leq 0.6$, the contribution of extragalactic UHECRs dominates at $E \sim E_{GZK}$, whereas at both less and larger energies the contribution of galactic sources becomes more important. This means that the anisotropy of angular distribution of UHECRs depends upon their energy and, for the Top-Down model with spectra under discussion, it is minimal at $E \sim E_{GZK}$.

In this paper we recalculate the contribution of the extragalactic component of UHECR for different life-time, masses of the SHDM particles $10^{12} \text{GeV} \leq m_X \leq 10^{19} \text{GeV}$, and spectra of injected proton. We show that the relative contributions of galactic and extragalactic

components of high energy protons depend upon these factors. For the most interesting models, the extragalactic component is found to be dominant at $E \sim E_{GZK}$ and the expected flux is well consistent with observations. The expected angular distribution on the sky of observed UHECR flux depends upon the energy of protons near the GZK cutoff and its variations should be considered as an important test for the Top-Down models.

Some cosmological manifestations of decays of SHDM particles can also be observed. In particular, decays of SHDM particles with masses $m_X \sim 10^{19}$ GeV can delay the recombination of hydrogen at redshifts $z \sim 1000$. This inference is especially important for discussion of the Cosmic Microwave Background (CMB) anisotropy and polarization power spectra. The same decays can increase the hydrogen ionization at smaller redshifts and accelerate the formation of first population of stars and galaxies. These manifestations can be tested with both available and future measurements of the CMB anisotropy and polarization.

The paper is organized as follows. In section 2 we discuss the spectra of extragalactic protons for different spectra of injected protons, in section 3 the combined flux of galactic and extragalactic sources is compared with observations. In section 4 we discuss the possible delay of hydrogen recombination due to decays of the SHDM particles. Main results are discussed in section 4.

II. EXPECTED SPECTRUM OF HIGH ENERGY PROTONS

In this paper we use the continual energy loss (CEL) approximation and describe the evolution of the number density of high energy extragalactic protons by the following equation [6]:

$$\frac{\partial N(E, t)}{\partial t} + 3H(t)N + \frac{\partial}{\partial E} \left(N \frac{dE}{dt} \right) = I(E, t), \quad (1)$$

$$\frac{1}{E} \frac{dE}{dt} = -H + H_0 \beta(E), \quad \beta(E) = \beta_\gamma(E) + \beta_\pi(E), \quad (2)$$

$$I = \omega_p \frac{n_0}{\tau_0} (1+z)^3 S(E), \quad H = -\frac{1}{1+z} \frac{dz}{dt} = H_0 (1+z)^{3/2},$$

where E and $N(E, t)$ are the energy and number density of protons per unit of energy, $H(t)$ is the Hubble constant, $H_0 = 100 h$ km/s/Mpc = 75 km/s/Mpc, z is a redshift, the functions $I(E, t)$ and $S(E)$ characterize the intensity and spectrum of injected protons, $\omega_p n_0 / \tau_0$ is the intensity of proton production at $z = 0$, functions $\beta_\gamma(E)$ and $\beta_\pi(E)$ describe the proton energy losses due to electron-positron pairs and photo-pions production and $\omega_p \sim 0.05$ is the fraction of protons in the SHDM particles decay.

The general solution of equation (1) is

$$N_{ex}(E_0, t_0) = \int_1^\infty \frac{dx}{x^4} \frac{E}{E_0} \frac{x^{-1} + \beta(E)}{1 + \beta(E_0)} \frac{I(E, x)}{H(x)} = \frac{\omega_p n_0}{H_0 \tau_0} \int_1^\infty \frac{dx}{x^{5/2}} \frac{E}{E_0} \frac{x^{-1} + \beta(E)}{1 + \beta(E_0)} S(E(x)), \quad (3)$$

where $E = E(x)$, $E_0 = E(z = 0)$, $t_0 = t(z = 0)$. This means that, in fact, the observed flux of extragalactic UHECRs depends upon the functions $\beta(E)$ and $S(E)$.

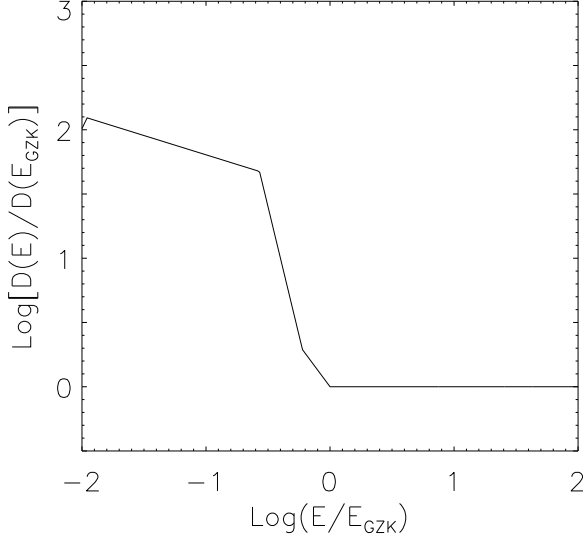


FIG. 1. The function $D(E)/D(E_{GZK})$ versus $\epsilon = E/E_{GZK}$ for photo-pion production.

A. Energy losses of protons

For protons with $E \geq E_{GZK}(1+z)^{-1}$, the free path, $D(E)$, is determined by photo-pion production on CMB photons. Following [21] we approximate this energy loss by the function:

$$\beta_\pi = (1+z)^3 \kappa_\pi, \quad (1+z)\epsilon \geq 1, \quad (4)$$

$$\beta_\pi = (1+z)^3 \kappa_\pi \epsilon^{p_1}, \quad 1 \geq (1+z)\epsilon \geq \epsilon_1, \quad (5)$$

$$\beta_\pi = (1+z)^3 \kappa_\pi \epsilon^{p_2} \epsilon_1^{p_1 - p_2}, \quad \epsilon_1 \geq (1+z)\epsilon \geq \epsilon_2, \quad (6)$$

$$\beta_\pi = (1+z)^3 \kappa_\pi \epsilon^{p_3} \epsilon_1^{p_1 - p_2} \epsilon_2^{p_2 - p_3}, \quad \epsilon_2 \geq (1+z)\epsilon, \quad (7)$$

$$\epsilon_1 \approx 0.6, \quad \epsilon_2 \approx 0.27, \quad p_1 \approx 1.3, \quad p_2 \approx 4, \quad p_3 \approx 0.3,$$

$$\epsilon = E/E_{GZK}, \quad E_{GZK} \approx 1.5 \cdot 10^{20} \text{ eV},$$

$$\kappa_\pi = \frac{cH_0^{-1}}{D(E_{GZK})} \approx 160, \quad D(E_{GZK}) = 25 \text{ Mpc}.$$

where the redshift dependence of density and temperature of CMB is taken into account. The function $\beta(E_{GZK})/\beta(E) = D(E)/D(E_{GZK})$ is plotted in Fig. 1.

For $E \ll E_{GZK}$, the energy losses due to e^+e^- pair production dominates (for review, see [21]) and

$$\beta_\gamma \approx 0.005(1+z)^3 \kappa_\pi. \quad (8)$$

For these functions $\beta(E)$, the redshifts variations of the proton energy can be found analytically as follows:

$$E(z_2) = E(z_1) \frac{1+z_2}{1+z_1} G_e(z_1, z_2), \quad \beta(E) = \kappa = \text{const}, \quad (9)$$

$$G_e(z_1, z_2) = \exp\left(\frac{2}{3} \kappa [(1+z_2)^{3/2} - (1+z_1)^{3/2}]\right),$$

$$E(z_2) = E(z_1) \frac{1+z_2}{1+z_1} G_p(z_1, z_2), \quad \beta(E) = \kappa \epsilon^p, \quad (10)$$

$$G_p^{-p}(z_1, z_2) = 1 - \kappa \frac{p \epsilon^p(z_1)}{p + 3/2} (1+z_1)^{3/2} \left[\left(\frac{1+z_2}{1+z_1} \right)^{p+3/2} - 1 \right].$$

For $p \rightarrow 0$, $G_p(z_1, z_2) \rightarrow G_e(z_1, z_2)$ and the expression (10) becomes identical to (9).

B. Galactic and extragalactic UHECR protons

The high concentration of the SHDM particles within the halo of Galaxy generates the galactic component of UHECRs, N_{gal} . Its spectrum reproduces the spectrum of generated protons. The relative contribution of galactic and extragalactic components can be roughly estimated as follows:

$$N_{gal}(E) = \omega_p \frac{n_0}{\tau_0} \frac{r_g}{c} \delta_g S(E) = \zeta_{gal} \frac{\omega_p n_0}{H_0 \tau_0} S(E), \quad (11)$$

$$\zeta_{gal} \sim \frac{H_0 r_g}{c} \delta_g = 3 \frac{r_g}{10^2 \text{ kpc}} \frac{\delta_g}{10^5} \quad (12)$$

where r_g is the radius of galactic halo.

More refined analysis [6] uses expected CDM density within the Galaxy and energy dependence of proton free path, $D(E)$. It extends the range of possible ratio of galactic to extragalactic components up to $\zeta_{gal} \sim 30 - 50$. Further on for comparison of galactic and extragalactic fluxes, we will take $\zeta_{gal} \sim 10$.

Both the observed fluxes and relative contributions of galactic and extragalactic components depend upon the spectrum of injected protons, $S(E)$. To illustrate this dependence we consider the normalized power spectra with exponents $\alpha \geq 1$ and $\alpha \leq 1$ and the log-normal spectrum proposed in [13].

Spectrum with $\alpha = 1.5 > 1$ and $E_{min} \ll E \leq E_{inj}$,

$$S_{pw}(E) = \frac{\alpha - 1}{E_{min}} \left(\frac{E}{E_{min}} \right)^{-\alpha} \left(1 - \frac{E}{E_{inj}} \right)^2, \quad (13)$$

is usually used to describe the decay of particles with moderate masses. It is model dependent and its applicability to the decay of extremely massive X-particles is in question (see, e.g., discussion in [13]). For such spectrum, using (3), we obtain

$$N_{ex} = \frac{\omega_p n_0}{H_0 \tau_0} \frac{\alpha - 1}{E_{min}} \left(\frac{E_0}{E_{min}} \right)^{-\alpha} \nu(E_0, \alpha). \quad (14)$$

The dimensionless function $\nu(E_0, \alpha)$ weakly depends upon α and describes how the flux of extragalactic protons varies with energy at $E_0 \sim E_{GZK}$. Numerically, $\nu(E_{GZK}, 1.5) \approx 10^{-2}$.

As is seen from (14) in this case both spectra of extragalactic and galactic protons are similar and the contribution of extragalactic component to the observed fluxes of UHECR is small, because $\nu \ll \zeta_{gal}$.

Spectra of injected protons with $\alpha \leq 1$,

$$S_{pw}(E) = \frac{c(\alpha)}{E_{inj}} \left(\frac{E}{E_{inj}} \right)^{-\alpha} \left(1 - \frac{E}{E_{inj}} \right)^2, \quad (15)$$

$$c(\alpha) = 0.5(1 - \alpha)(2 - \alpha)(3 - \alpha),$$

seem to be more promising. For such spectra with $\alpha \leq 0.6$ and $E_{inj} \geq 10^2 E_{GZK}$, we have almost universal spectrum of extragalactic protons,

$$N_{ex}(E_0) = \frac{\omega_p n_0}{H_0 \tau_0} E_0^{-1} \mu(E_0, E_{inj}, \alpha), \quad (16)$$

$$\mu(E_{GZK}, E_{inj}, \alpha) \approx 5 \cdot 10^{-3}. \quad (17)$$

Dimensionless function $\mu(E_0, \alpha)$ weakly depends upon E_{inj} and α and describes variations of the flux of extragalactic protons with energy at $E_0 \sim E_{GZK}$. For such spectra of injected protons galactic component dominates only at high energy when

$$\left(\frac{E_0}{E_{inj}} \right)^{1-\alpha} \geq \frac{\mu(E_0, E_{inj}, \alpha)}{c(\alpha) \zeta_{gal}}. \quad (18)$$

We consider also the log-normal spectra of injected protons recently proposed in [13] (see also [6]),

$$S_{ln}(E) = \frac{1}{\sqrt{2\pi} E \sigma_{inj}} \exp \left(-\frac{\ln^2(E/E_{inj})}{2\sigma_{inj}^2} \right), \quad (19)$$

with $\sigma_{inj} = 3 - 7$ and the same two energies of injection as above. In this case the spectrum of extragalactic protons is also almost universal and similar to (16) with a similar function $\mu(E_0, E_{inj}, \sigma_{inj})$. For such spectrum, the contribution of galactic sources is shifted to energy $E_0 \sim E_{inj} \exp(-\sigma_{inj})$ and dominates only at high energy when

$$\ln^2 \left(\frac{E_0}{E_{inj}} \right) \leq 2\sigma_{inj}^2 \ln \left(\frac{\zeta_{gal}}{\sqrt{2\pi} \mu \sigma_{inj}} \right). \quad (20)$$

III. EXPECTED FLUX OF UHECR PROTONS FOR TOP-DOWN MODELS

Here we consider the Top-Down models for two injection energy, $E_{inj} = 10^2 E_{GZK}$ and $E_{inj} = 10^8 E_{GZK}$. The first model is related to decays of SHDM particles with moderate masses often discussed in literature (see, e.g., [6,7]). The second model describes the decay of ultra massive particles such as, for example, explosive evaporation of black hole remnants discussed in Dolgov, Naselsky & Novikov [20].

To illustrate the influence of the life - time of the SHDM particles, τ_0 , we consider two models, one with τ_0 larger than the age of the Universe, $T_U \sim H_0^{-1}$, and other with $\tau_0 \approx 0.1 T_U$.

The normalized expected fluxes of UHECR protons,

$$F(\epsilon_0) = \frac{dJ(E_0)}{dE_0} \frac{E_0^3}{10^{24} e V^2 m^{-2} ster^{-1} s^{-1}} \quad (21)$$

are plotted in Figs. 2 - 5 versus $\epsilon_0 = E_0/E_{GZK}$ together with available observational data. We show the fluxes of extragalactic component alone and combined fluxes for extragalactic and galactic components for $\zeta_{gal}=10$.

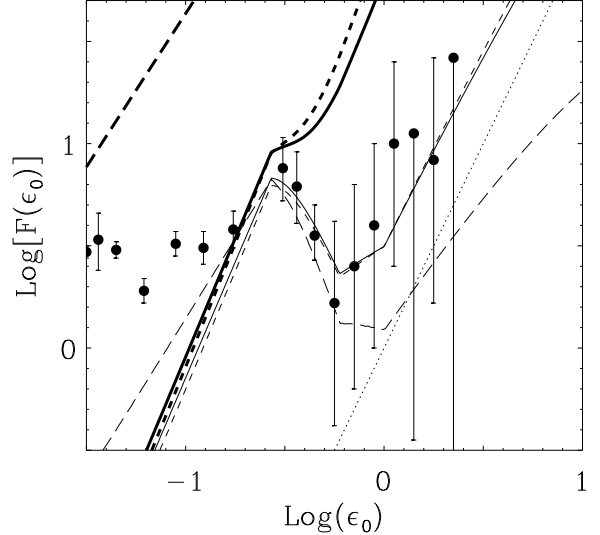


FIG. 2. The functions $F(\epsilon_0)$ (21) versus $\epsilon_0 = E/E_{GZK}$ are plotted for long-lived SHDM particles with $\tau_0 \gg T_U$, $E_{inj}/E_{GZK} = 10^2$, and power spectra of injected protons with $\alpha = 1.5$ (long dashed line), $\alpha = 0.5$ (solid line), and $\alpha = 0.25$ (dashed line). Thin lines show the contribution of extragalactic component alone, thick lines show the contribution of extragalactic and galactic sources for $\zeta_{gal} = 10$. The observed fluxes are plotted by points. For comparison, the flux $dJ/dE_0 \propto E_0^{-1}$ is plotted by dotted line.

A. Models with power spectra of injected protons

As was noted above, for power spectra (13) with larger exponent $\alpha = 1.5 \geq 1$, the contribution of extragalactic

component, $N_{ex}(E_0)$, weakly depends upon the energy of injection and is negligible in comparison with the contribution of the galactic component. These results are a natural consequence of predominant generation of lower energy protons in such models. Of course, for suitable choice of decay rate, n_0/τ_0 , the galactic component can explain the observed growth of flux at $E \geq E_{GZK}$.

1. Models with $\alpha \leq 1$ and larger life-time of the SHDM particles, $\tau_0 \gg T_U$

For models with smaller exponents, $\alpha = 0.5$ and 0.25 , and moderate energy of injection, $E_{inj} = 10^2 E_{GZK}$, plotted in Fig. 2, the resulting flux is sensitive to the contribution of galactic component and, for the most interesting energies $E_0 \geq 0.2 - 0.3 E_{GZK}$, the impact of extragalactic component becomes noticeable only for $\zeta_{loc} \leq 1$. These results agree with approximate estimates (18).

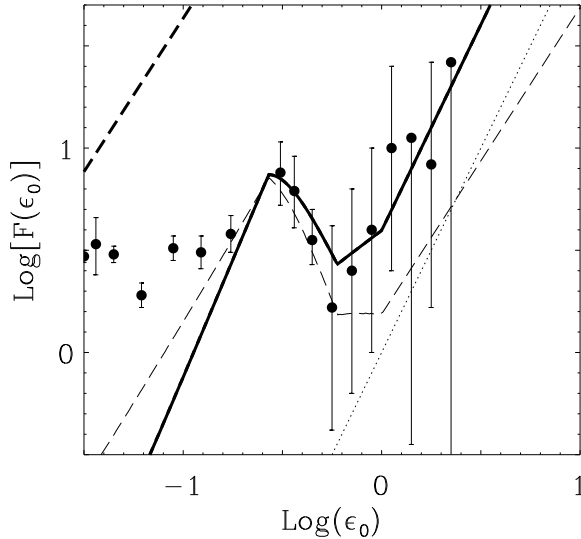


FIG. 3. The functions $F(\epsilon_0)$ (21) versus $\epsilon_0 = E/E_{GZK}$ are plotted for long-lived SHDM particles with $\tau_0 \gg T_U$, $E_{inj}/E_{GZK} = 10^8$, and power spectra of injected protons with $\alpha = 1.5$ (long dashed line), $\alpha = 0.5$ (solid line), and $\alpha = 0.25$ (dashed line). Thin lines show the contribution of extragalactic component alone, thick lines show the contribution of extragalactic and galactic sources, for $\zeta_{gal} = 10$. The observed fluxes are plotted by points. For comparison, the flux $dJ/dE_0 \propto E_0^{-1}$ is plotted by dotted line.

For models with high energy of injection, $E_{inj} = 10^8 E_{GZK}$, and with smaller exponents, $\alpha = 0.5$ and 0.25 , the expected spectrum of extragalactic component is similar to (16), and the resulting flux is weakly sensitive to the contribution of the galactic component. For the most interesting energies, $E_0 \sim E_{GZK}$, the extragalactic component dominates, at least for $\zeta_{gal} \leq 30$.

Results plotted in Fig. 3 show that, for suitable decay rate,

$$\omega_p n_0 / \tau_0 \approx 10^{-46} \text{cm}^{-3} \text{s}^{-1}, \quad (22)$$

such models reproduce quite well the observed fluxes of UHECR with energies $E \geq 0.1 E_{GZK}$.

2. Models with shorter life-time of the SHDM particles

In models with shorter life – time of the SHDM particles, $\tau_0 \sim 0.125 T_U$, the number density of SHDM particles rapidly decreases with time due to their progressive decays what, in turn, increases the contribution of extragalactic component for $0.1 \leq E_0/E_{GZK} \leq 1$. In spite of this, for models with moderate energy of injection, $E_{inj} = 10^2 E_{GZK}$, this factor cannot essentially amplify the contribution of extragalactic component and it becomes noticeable only for $\zeta_{gal} < 10$.

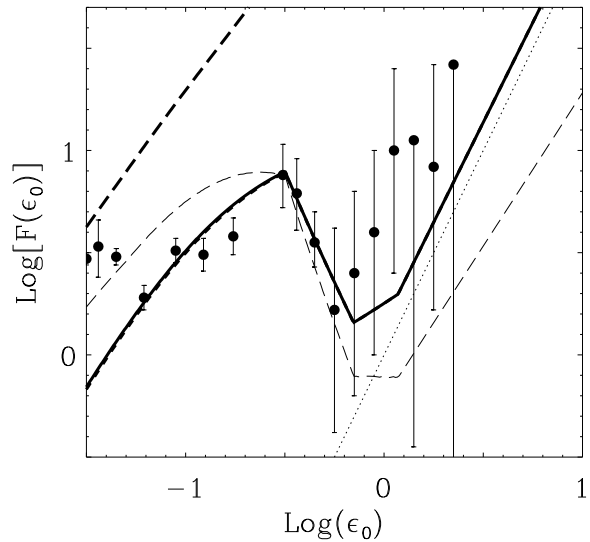


FIG. 4. The functions $F(\epsilon_0)$ (21) versus $\epsilon_0 = E/E_{GZK}$ are plotted for short-lived SHDM particles with $\tau_0 = 0.125 T_U$, $E_{inj}/E_{GZK} = 10^8$, and power spectra of injected protons with $\alpha = 1.5$ (long dashed line), $\alpha = 0.5$ (solid line), and $\alpha = 0.25$ (dashed line). Thin lines show the contribution of extragalactic component alone, thick lines show the contribution of extragalactic and galactic sources, for $\zeta_{gal} = 10$. The observed fluxes are plotted by points. For comparison, the flux $dJ/dE_0 \propto E_0^{-1}$ is plotted by dotted line.

However, for models with ultra – high energy of injection, $E_{inj} = 10^8 E_{GZK}$, and smaller exponents, $\alpha = 0.5$ and $\alpha = 0.25$, results plotted in Fig. 4 for $\tau_0 = 0.125 T_U$, demonstrate that, for $E_0 \geq 0.06 E_{GZK}$, the extragalactic component dominates. For the decay rate

$$\frac{\omega_p n_0}{\tau_0} \approx 0.3 \cdot 10^{-46} \text{cm}^{-3} \text{s}^{-1}, \quad n_0 \sim \omega_p^{-1} 10^{-30} \text{cm}^{-3}, \quad (23)$$

it reproduces quite well the observed flux of UHECR for energy $E \geq 0.06 E_{GZK}$. If SHDMs are identified with

primordial black holes with $M_{pbh} \sim 10^{-5}g$ then the mean densities of SHDMs at $z = 0$ and at $z \gg 1$ are

$$\rho(0) \sim \omega_p^{-1} 10^{-35} g \text{ cm}^{-3}, \quad (24)$$

$$\frac{\rho(z)}{(1+z)^3} \sim \omega_p^{-1} (10^{-31} - 10^{-32}) g \text{ cm}^{-3} \leq \rho_{cr}, \quad (25)$$

respectively.

B. Models with log-normal spectra of injected protons

For log-normal spectra of injected protons, S_{ln} , (19), with moderate dispersions $\sigma_{inj} = 5$ and energies of decays $E_{inj} = 10^2 E_{GZK}$ and $E_{inj} = 10^8 E_{GZK}$, the resulting fluxes of UHECRs, for $\zeta_{gal} = 10$, are plotted in Fig. 5. For models with larger E_{inj} , the expected flux at $E_0 \sim E_{GZK}$ is dominated by the extragalactic component and reproduces the observed flux variations. In contrast, for models with smaller E_{inj} the expected flux is dominated by the galactic component and is far from the observed one. The contribution of galactic sources at $E_0 \sim E_{GZK}$ depends upon ζ_{gal} and rapidly decreases for larger E_{inj} and smaller σ_{inj} .

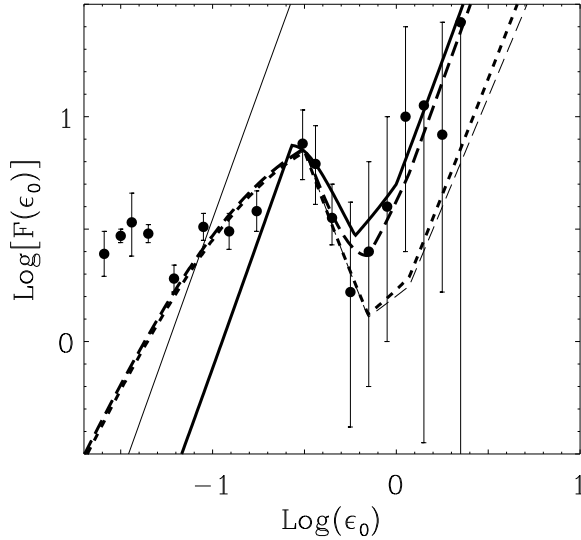


FIG. 5. The functions $F(\epsilon_0)$ (21) versus $\epsilon_0 = E/E_{GZK}$ are plotted for log-normal spectra of injected protons with the life-time $\tau_0 \gg T_U$, $\sigma_{inj} = 5$ for $E_{inj} = 10^2 E_{GZK}$ (thin solid line) and $E_{inj} = 10^8 E_{GZK}$ (thick solid line). For $\tau_0 \approx 0.125 T_U$, $E_{inj} = 10^8 E_{GZK}$, the same function is plotted for $\sigma_{inj} = 5$ (dashed line) and $\sigma_{inj} = 7$ (long dashed line). The observed fluxes are plotted by points.

At $E \leq E_{GZK}$ the extragalactic flux is more sensitive to the life-time of SHDM particles. As is seen from Fig. 5 for the decay rate of SHDM particles (22) and longer life

-time, $\tau_0 \gg T_U$, the resulting fluxes, for $E_0 \geq 0.3 E_{GZK}$, describe quite well the observations. For shorter life-time, $\tau_0 \sim 0.1 T_U$, and the decay rate of SHDM particles (23), this fluxes reproduce well the observations up to $E_0 \sim 0.06 E_{GZK}$.

IV. SOME COSMOLOGICAL MANIFESTATIONS OF DECAYS OF SHDM PARTICLES

The injection of energy due to decays of SHDM particles during the "dark ages", at redshifts $10^3 \geq z \geq 10$, leads also to interesting consequences some of which can be tested with available and/or future observations. Such consequences were recently discussed by Peebles, Seager and Hu ([24]) in the framework of a simple toy model. Here we repeat this analysis using results obtained above.

The decays of SHDM particles produce, among others, many high energy photons and electron-positron pairs which, after reduction of their energy in electromagnetic cascades, are converted into $Ly-\alpha$ and $Ly-c$ photons with energies $E_\alpha = 10.2\text{eV}$ and $E_c = 13.6\text{eV}$, respectively. The efficiency of such conversion is small due to high complexity of these cascades. To avoid many assumptions required for discussion of the final intensity and spectrum of photons at energy of interest we will assume, following [24], that the decays of SHDM particles lead to creation of $Ly-c$ and $Ly-\alpha$ photons with a rate

$$\frac{dn_{ph}}{dt} \approx \varepsilon_{ph} \frac{E_{inj}}{E_\alpha} \frac{n_0}{\tau_0} \approx \left(\frac{1+z}{1000} \right)^3 \cdot 10^{-10} \frac{\varepsilon_{ph}}{\text{cm}^3 \text{s}}, \quad (26)$$

where, for numerical estimates, we use $E_{inj} = 10^8 E_{GZK} \approx 10^{28} \text{ eV}$, the decay rate $n_0/\tau_0 = 10^{-46} \text{ cm}^{-3} \text{ s}^{-1}$, and $\varepsilon_{ph} \ll 1$ characterizes the unknown efficiency of energy transformation to $Ly-c$ and $Ly-\alpha$ photons.

Comparing the rate of photons creation (26) with the rates discussed in [24],

$$\frac{dn_\alpha}{dt} = \varepsilon_\alpha n_H H \approx 2.5 \cdot 10^{-14} \left(\frac{1+z}{1000} \right)^{9/2} \frac{\varepsilon_\alpha}{\text{cm}^3 \text{s}}, \quad (27)$$

we see that, for $\varepsilon_\alpha \sim 1 - 10$ and correspondingly for

$$\varepsilon_{ph} \sim 3 \cdot 10^{-4} \varepsilon_\alpha \sim 10^{-4} - 10^{-3}, \quad (28)$$

the impact of discussed decays of SHDM particles effectively delays the recombination of hydrogen and leads to measurable distortions of the observed spectra of CMB fluctuations at angular wave numbers $l \geq 100 - 200$ (see detailed discussion in [24]).

For shorter life-time of SHDM particles, $\tau_0 \approx 0.125 T_U$, the decay rate at redshifts $z \geq 10$ increases by about a factor of 10^3 in comparison with (26) and wider range of E_{inj} and ε_{ph} can also be considered. The impact of the factor ω_p omitted in (26) will also reinforce these estimates.

At smaller redshifts, $z \leq 500$, generated Ly-c photons partly ionize neutral hydrogen. For small ionization degree of hydrogen, $x_H \leq 1$, all Ly-c photons are rapidly absorbed and x_H can be found from the equilibrium equation which describes the conservation of number of electrons and Ly-c photons together,

$$\frac{dn_{ph}}{dt} = \alpha_{rec}^* n_e n_p = \alpha_{rec}^* \langle n_b \rangle^2 x_H^2 \quad (29)$$

where $\alpha_{rec}^* \approx 2 \cdot 10^{-13} (T/10^4 K)$ is the recombination coefficient for states with the principle quantum number $n \geq 2$, $T/10^4 K \approx 0.03 [(1+z)/100]^2$ is the temperature of hydrogen under the condition of small ionization, $\langle n_b \rangle \approx 0.24 (\Omega_b h^2 / 0.02) [(1+z)/100]^3$ is the mean number density of baryons, and $n_p = n_e = x_H \langle n_b \rangle$. For simplicity, we neglected here the contribution of helium.

As follows from Eqs. (26) and (29), the expected degree of hydrogen ionization is

$$x_H \approx \sqrt{\varepsilon_{ph}} \left(\frac{1+z}{100} \right)^{-3/4}. \quad (30)$$

For $\varepsilon_{ph} \geq 10^{-6}$, this degree is higher than the degree of remaining hydrogen ionization after recombination, $x_H \sim 10^{-3}$. For shorter life - time of SHDM particles, $\tau_0 \approx 0.125 T_U$, the decay rate at redshifts of interest grows by about a factor of 10^3 and increases the ionization degree up to

$$x_H \sim \sqrt{10^3 \varepsilon_{ph}} \left(\frac{1+z}{100} \right)^{-3/4}, \quad (31)$$

that again essentially extends the range of acceptable E_{inj} and ε_{ph} .

The considered growth of x_H , at redshifts $z \leq 500$, does not increase significantly the optical depth for Thompson scattering, τ_T , because

$$\frac{d\tau_T}{dz} \propto x_H (1+z)^{-3/2}.$$

So, it does not amplify perturbations of the observed spectra of CMB fluctuations as compared with distortions generated at redshifts $z \sim 1000$. But this growth essentially accelerates the creation of molecules H_2 and therefore formation and cooling of first galaxies.

These results were obtained when the extragalactic component of UHECR, discussed in Sec. III, dominates. These estimates can be also repeated for decays of more massive SHDM particles and usually discussed spectra of injected protons, with $\alpha = 1.5$ and $n_0/\tau_0 \sim 10^{-46} cm^{-3} s^{-1}$.

V. SUMMARY AND DISCUSSION

Available information about possible properties of SHDM particles and, in particular, about their life -

time, energy and spectra of injected protons is now very limited, and, in fact, the analysis of UHECR can be considered as an experimental test for particle interactions at ultra - high energy. Results obtained in previous Sections show that under quite natural assumptions about the energy, life-time and spectrum of injected protons, a reasonable explanation of the observed fluxes of UHECR can be achieved. The CEL approximation used in this paper describes quite well the expected fluxes at $E \leq E_{GZK}$ but, for larger energies, the observed fluxes can be essentially distorted due to random character of energy losses above the GZK cutoff [22].

For both log-normal and power spectra of injected protons, S_{ln} (19) and S_{pw} (15), with $E_{inj} \geq 10^5 E_{GZK}$ and $\alpha \leq 1$, and for suitable intensity of proton creation and life - time of SHDM particles, our results are consistent with the observed fluxes for $E_0 \geq 0.06 E_{GZK}$. They demonstrate that, for $E_0 \sim E_{GZK}$, the observed flux of UHECR can be mainly related to the extragalactic component. For such spectra of injected protons, the expected flux is found to be moderately sensitive to assumptions about the galactic sources, the energy of injection for $E_{inj} \geq 10^5 E_{GZK}$ and to values of $\alpha \leq 0.6$ and $\sigma_{inj} \leq 10$ for power and log-normal spectra, respectively. In contrast, for the models with power spectra and $\alpha \geq 1$ (13), and for models with smaller energy of injection, $E_{inj} \sim 10^2 - 10^3 E_{GZK}$, the contribution of extragalactic component of UHECR is small, the galactic component dominates and the observed fluxes cannot be reproduced.

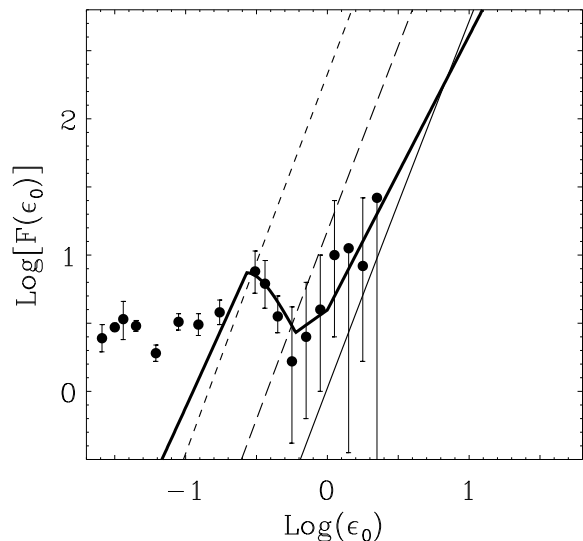


FIG. 6. The functions $F(\epsilon_0)$ (21) versus $\epsilon_0 = E/E_{GZK}$ are plotted for log-normal spectra of injected protons with the life - time $\tau_0 \gg T_U$, $\sigma_{inj} = 5$ and $E_{inj} = 10^8 E_{GZK}$. The extragalactic component is plotted by thick solid line, the galactic components are plotted for $\zeta_{gal} = 10$ (solid line), $\zeta_{gal} = 30$ (long dashed line) and $\zeta_{gal} = 100$ (dashed line).

For models under consideration with ultra - high energy of injection, the observed fluxes for $E_0 \sim 0.1 -$

$10E_{GZK}$ are mainly related to the almost isotropic extragalactic component generated at redshifts $z \leq 0.1-0.2$. At smaller and larger energies domination of the galactic component leads to an essential growth of anisotropy. This means that the anisotropy of angular distribution of observed UHECR is expected to be minimal for the energy range $E_0 \sim 0.1 - 10E_{GZK}$.

To illustrate this statement we plot in Fig.6 the galactic and extragalactic fluxes separately for log-normal spectrum of injected protons for three values of ζ_{gal} . As is seen from this Fig., for $\zeta_{gal} \leq 30$ more isotropic extragalactic component dominates at $E \leq 1-10E_{GZK}$ while for $\zeta_{gal} \geq 30$ stronger anisotropy will be generated for all energies by the dominant galactic component. These variations of the anisotropy allow to test these versions of the Top - Down models.

For simplicity and due to qualitative character of our analysis, we consider the CDM dominated flat cosmological model only. Evidently, these results can be recalculated in the same manner for other cosmological models and, in particular, for the most popular Λ CDM flat model. Of course, for such cosmological models some of the parameters used here will be changed. However, even for such models the main qualitative results concerning the influence of the life - time, mass and spectra of injected protons will remain.

The discussed cosmological manifestations of the Top-Down model of UHECR generation provide an indirect test of this model. As is seen from evaluations given in Sec. IV for the high masses of SHDM particles and energy of injection $E_{inj}/E_{GZK} \sim 10^8$, the effective delay of the cosmological recombination is possible for reasonable values of efficiency of creation of Layman photons. For models with decays of vortons, necklaces and other particles with $E_{inj}/E_{GZK} \ll 10^8$ these cosmological manifestations are negligible.

The expected distortions of CMB fluctuations due to delayed recombination can be directly tested with the available modern balloon-born experiments (MAXIMA-1 [25] and BOOMERANG [26]) and future - MAP and PLANCK satellite missions - by measuring the CMB anisotropy and polarization power spectra. These problems will be discussed elsewhere.

ACKNOWLEDGMENT

Authors are grateful to P. Chardonnet , M. Demianski and I. Novikov for discussions and help during the preparation of the paper. This paper was supported in part by Danmarks Grundforskningsfond through its support for the establishment of the Theoretical Astrophysics Center, by grants RFBR 17625 and INTAS 97-1192.

- [1] K. Greisen, Phys. Rev. Lett., **16**, 748, 1966.
- [2] G.T. Zatsepin and V.A. Kuzmin, Pis'ma Zh. Eksp.Theor.Fiz., **4**, 114, 1966; JETP. Lett., **4**, 78, 1966.
- [3] N. Hayashida et al., Phys.Rev.Lett, **73**, 3491, 1994; S. Yoshida et al., Astropart.Phys., **3**, 105, 1995; M. Takeda et al., Phys. Rev. Lett., **81**, 1163, 1998; see also <http://icrsun.isrr.u-tokyo.ac.jp/as/project/agasa.html>
- [4] S. Yoshida and H. Dai, J.Phys.G, **24**, 905,1998.
- [5] M.A. Lawrence, R.J.O. Reid and A.A. Watson, J.Phys.G., Nucl.Part.Phys., **17**, 733, 1991; <http://ast.leeds.ac.uk/haverah/hav-home.html>.
- [6] P. Bhattacharjee and G. Sigl, Phys.Rept., **327**, 109, 2000.
- [7] M. Birkel and S. Sarkar, Astropart.Phys., **9**, 297, 1998.
- [8] V.S. Berezinsky, M.Kashelrieß and A.Vilenkin, Phys.Rev.Lett, **79**, 4302, 1997.
- [9] V.A.Kuzmin and V.A.Rubakov, Yader.Fiz., **61**, 1122, 1998.
- [10] V.S. Berezinsky, Nuclear Phys. B (Proc.Suppl.), **87**, 387, 2000.
- [11] L.Kofman, A.Linde and A.Starobinsky, Phys.Rev.Lett., **73**, 3195, 1994.
- [12] C.T. Hill, D.N. Shramm and T.P. Walker, Phys.Rev.D, **36**, 1007, 1987; P. Bhattacharjee and N.C. Rana, Phys.Lett.B, **246**, 365, 1990; G. Vincent, N. Antunes and M. Hindmarsh, Phys.Rev. Lett., **80**, 2277, 1998. U.F. Wichoski, R.H. Brandenberger and J.H. MacGibbon, hep-ph/9903545.
- [13] V.S. Berezinsky and M. Kashelrieß, hep - ph/0009053.
- [14] C.T. Hill, Nucl.Phys.B, **224**, 469, 1983.
- [15] V. Berezinsky, X. Martin and A. Vilenkin, Phys.Rev.D, **56**, 2024, 1997.
- [16] V. Berezinsky and A. Vilenkin, Phys.Rev.Lett., **79**, 5202, 1997.
- [17] L. Masperi and G. Silva, Astrop.Phys., **8**, 173, 1998.
- [18] J.H. MacGibbon, Nature, **329**, 308, 1987.
- [19] J.D. Barrow, E.J. Copeland, A.R. Liddle, Phys.Rev.D, **46**, 645, 1992,
- [20] A. Dolgov, P. Naselsky and I. Novikov, astro-ph/0009470.
- [21] P. Blasi, Phys.Rev.D, **60**, 023514, 1999.
- [22] A. Achterberg, Y. Gallant , C.A. Norman and D.B. Melrose, astro-ph/9907060.
- [23] G.R. Farrar and T. Piran, astro-ph/0010370.
- [24] P.J.E. Peebles, S. Seager and W. Hu, astro-ph/0004389.
- [25] S. Hanany et al. astro-ph/0005123, 2000.
- [26] P. De Beranrdis et al. Nature, **404**, 955, 2000.